BMC Musculoskeletal Disorders

RESEARCH

Open Access

Effect of bisphosphonate on bone microstructure, mechanical strength in osteoporotic rats by ovariectomy

Yuzhu Wang[1†], Zhanglin Wu[2†], Chun Li[1], Chenhao Ma[1], Jingyang Chen[1], Mincong Wang[2*], Dawei Gao[1], Yufeng Wu[1] and Haibin Wang[3]

Abstract

Background Bisphosphonate (BP) can treat osteoporosis and prevent osteoporotic fractures in clinical. However, the effect of BP on microstructure and mechanical properties of cortical and trabecular bone has been taken little attention, separately.

Methods In this study, BP was used to intervene in ovariectomized female SD rats. The femoral micro-CT images were used to measure the structural parameters and reconstruct the 3D models in volume of interest. The structural parameters of cortical and trabecular bone were measured, and the mechanical properties were predicted using micro-finite element analysis.

Results There was almost no significant difference in the morphological structure parameters and mechanical properties of cortical bone between normal, ovariectomized (sham-OVX) and BP intervention groups. However, BP could significantly improve bone volume fraction (BV/TV) and trabecular separation (Tb.SP) in inter-femoral condyles (IT) (sham-OVX vs. BP, $p < 0.001$), and had no significant effect on BV/TV in medial and lateral femoral condyles (MT, LT). Similarly, BPs could significantly affect the effective modulus in IT (sham-OVX vs. BP, $p < 0.001$), and had no significant difference in MT and LT. In addition, the structural parameters and effective modulus showed a good linear correlation.

Conclusion In a short time, the effects of BP intervention and osteoporosis on cortical bone were not obvious. The effects of BP on trabecular bone in non-main weight-bearing area (IT) were valuable, while for osteoporosis, the main weight-bearing area (MT, LT) may improve the structural quality and mechanical strength of trabecular bone through exercise compensation.

Keywords Bisphosphonate, Bone microstructure, Mechanical strength, Osteoporosis

†Yuzhu Wang and Zhanglin Wu contributed to the work equally.

*Correspondence:
Mincong Wang
Mincong1215@sina.com

[1]Department of Orthopaedic Surgery, Zhongshan Hospital of Traditional Chinese Medicine, Guangzhou University of Traditional Chinese Medicine, Zhongshan, Guangdong 528401, China
[2]Department of Orthopaedic Surgery, The Fifth Affiliated Hospital of Southern Medical University, Guangzhou, Guangdong 510920, China
[3]Department of Orthopaedic Surgery, First Affiliated Hospital, Guangzhou University of Chinese Medicine, Guangzhou, Guangdong 510405, China

Introduction

Osteoporosis (OP) is a major age-related bone disease, its main characteristic is the decrease of bone tissue density and the abnormal change of bone microstructure, which leads to the decrease of bone strength and the easy occurrence of fracture [1]. Osteoporosis leads to the destruction of trabecular structure and thinning of trabecular bone, in patients with osteoporosis, the bone trabeculae become irregular and the gaps increase, resulting in a loose and fragile bone structure [2]. Decreased bone density and changes in bone microstructure caused by osteoporosis can significantly reduce bone strength and stress resistance. Osteoporosis increases the risk of fracture by affecting bone microstructure and bone strength, and the prevention and treatment of osteoporosis is very important [3].

Bisphosphonate (BP), a drug commonly used to treat osteoporosis, reduce bone loss primarily by inhibiting the activity of bone-absorbing cells (osteoclasts) [4], thereby, increasing bone density and reducing the risk of fractures. It is widely used to treat conditions such as osteoporosis, bone metastases and hypercalcemia [5]. Studies have confirmed that BP can significantly reduce the incidence of fractures, especially vertebral fractures and hip fractures, which are the most common complications in patients with osteoporosis. It can also improve patients' quality of life, reduce bone pain and improve exercise capacity [6].

With the continuous development of imaging technology, high-resolution micro-computed tomography (micro-CT/μ-CT) with a resolution of up to microns now plays an important role in the application and development of imaging technology, especially in the research field of small animal specimens and large animal ex vivo specimens. Micro-CT has become the "gold standard" for evaluating bone morphology and bone microstructure [7]. Micro-CT has high spatial resolution, relatively low cost, easy to use. It can obtain detailed three-dimensional spatial structure information inside the tissue [8]. Using powerful image processing software, researchers can observe the sectional images from any angle, which is very suitable for quantitative analysis of bone microstructure changes caused by bone metabolic diseases [9].

As for the biomechanical evaluation of osteoporosis after treatment, finite element analysis can be used to evaluate the changes of bone density and bone strength after treatment of osteoporosis [10], especially in combination with high-resolution CT images, which can efficiently predict the strength changes of trabecular bone [11]. However, in previous studies, few studies have paid attention to the degree of influence of osteoporosis on trabecular and cortical bone separately, and the degree of improvement of bisphosphonates on trabecular and cortical bone.

In this study, the biomechanical effect of osteoporosis and BP on trabecular and cortical bone separately were evaluated using micro-CT images to calculate the microstructural parameters and micro-CT based finite element method (μ-FEM) to predict the mechanical strength of cortical and trabecular bones in different groups, finally, the correlation relationship of measured structural parameters and mechanical strength was discussed.

Methods and materials

Osteoporotic animal models and bisphosphonate intervention

The animal research protocol was approved by the ethics committee of Zhongshan Hospital of Traditional Chinese Medicine Affiliated to Guangzhou University of Traditional Chinese Medicine (NO. AEWC-2023008) with use license available (SYXK 2020−0109). A total of 30, 2-month-old female Sprague−Dawley (SD) rats were obtained from Guangdong Medical Animal Laboratory Center (use license: SCXK 2022-0002) for medical research and randomly separated into normal group (Control, $n=10$), ovariectomized group (sham-OVX, $n=10$), and bisphosphonate group (BP, $n=10$). All rats were raised in a standard specific-pathogen-free (SPF) environment and allowed free access to food. After two weeks of adaptive feeding, the ovaries of the sham-OVX group and the BP group were removed after inhalation anesthesia using isoflurane (3% induction, then 2% maintenance, with oxygen) at the rate of 1.2 L/min, while the control group underwent skin incision without ovary removal. The ovariectomized rats were given bisphosphonate ((Jule Pharmaceutical Co, Chengdu, China. 0.2 g/tablet, the suspension prepared with distilled water to 20 g/L before use) after the osteoporotic models succeed (Fig. 1). After 12 weeks, all rats were euthanized using cervical dislocation, and the right femurs were dissected and collected. Soft tissues connected to the right femur and tibia were removed, the femurs were fixed with 4% paraformaldehyde and stored at room temperature (25 °C) for micro-CT scanning, the fresh tibias were compressed in a three-point bending test [12].

Micro-CT images of samples

The excised right femurs were scanned using a high-resolution micro-CT scanner (SkyScan1276, Bruker, USA) at a resolution of 10 μm, with a voltage of 80 kV, a current of 100 μA. Images were then reconstructed using bundled software CTAn to analyze the micro-structural parameters for trabecular and cortical bone [13]. The cortical bone with a thickness of 4.58 mm at the middle femoral shaft (MC) and 2.60 mm at the distal femoral shaft (DC), the trabecular bone with diameter of 1.28 mm, height of 1.50 mm at the inter-femoral condyles (IT), medial and lateral femoral condyles (MT, LT), were extracted

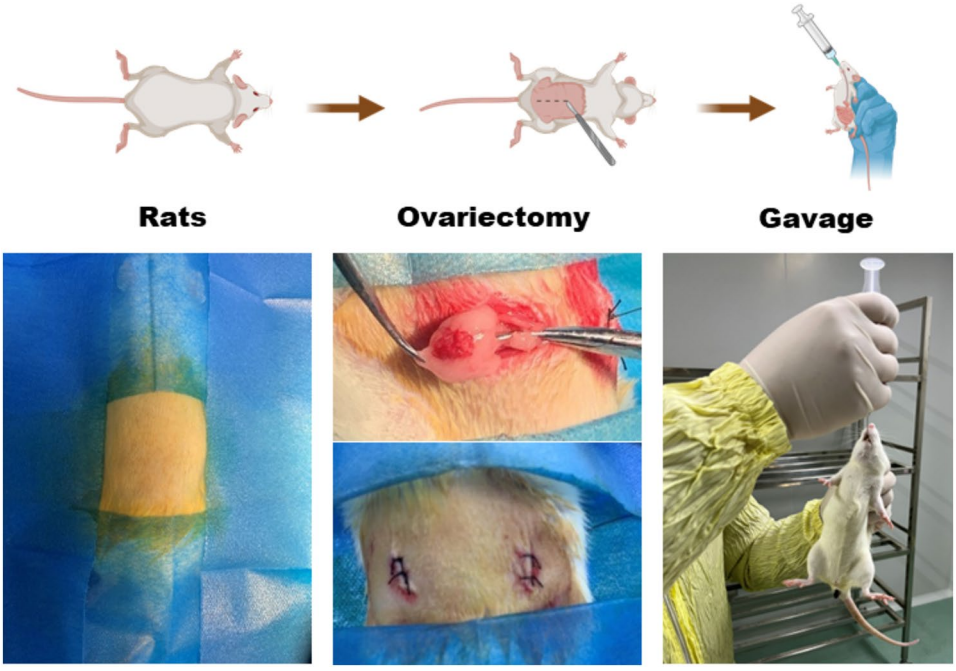

Fig. 1 Bilateral ovaries of female rats were removed and bisphosphonates were used to intervene osteoporosis rats

separately as VOI. In this study, the structural parameters for cortical bone with cortical thickness (Ct.Th, mm), cortical area (Ct.Ar, mm^2), total area (Tt.Ar, mm^2), the ratio of cortical area and total area (Ct.Ar/Tt.Ar), for trabecular bone with bone volume fraction (BV/TV), trabecular thickness (Tb.Th, mm), trabecular number (Tb.N, 1/mm), trabecular separation (Tb.Sp, mm), were measured [14].

Reconstruction of bone modeling in VOI

The original micro-CT images converted to Digital Imaging and Communications in Medicine (DICOM) format with another bundled software, DICOM images were imported into a medical image processing software program (Mimics 22, Materialise, Belgium), the 3D models of trabecular and cortical bone in VOI were reconstructed in different groups (Fig. 2). The "stl" files of VOI were transformed to the "step" files for finite element analysis. The porosity of trabecular bone in VOI was calculated using Eq. 1 (Table 1).

$$\Phi\ (\%) = (1 - {}^{\mathrm{BV}}\!/_{\mathrm{TV}}) \times\ 100 \tag{1}$$

where Φ, BV/TV are the porosity, bone volume/total volume, respectively.

Finite element modeling of VOI

To evaluate the mechanical properties of the trabecular bone, cortical bone of VOI, compression tests in silico were performed [15], axial displacement U_z= 0.5 mm was applied on the top rigid plate with an increment size of 0.01, and the bottom rigid plate was fixed in all directions. The stress-strain curves were used to obtain the effective elastic modulus using Eq. 2.

$$E_{effective} = \frac{\sigma}{\epsilon} = \frac{{}^{F_R}\!/_{A}}{{}^{\Delta h}\!/_{h}} \tag{2}$$

where F_R, A, Δ h, h are the reaction force, area, changed length, and the length of porous structure, respectively.

Finite element models were built in ABAQUS (ABAQUS 2020, Dassault Systems, Providence, RI). The initial elastic modulus of cortical bone was regarded as 13 GPa [16], the trabecular bone was assigned using Eq. 3, and the Poisson's ratio of 0.3 was used [17].

$$E = 14,899(BV/TV)^{1.94} \tag{3}$$

where E, BV/TV are the Young's modulus, bone volume/total volume, respectively.

The mesh sensitivity analysis and validation for finite element model had been performed in our previous studies [18, 19]. In the study, the mesh size was 0.1 mm for cortical bone and 0.01 mm for trabecular bone, C3D10 10-node quadratic tetrahedron elements were adopted, respectively. Totally, 150 finite element models including cortical and trabecular bone samples in different groups were analyzed (Fig. 3).

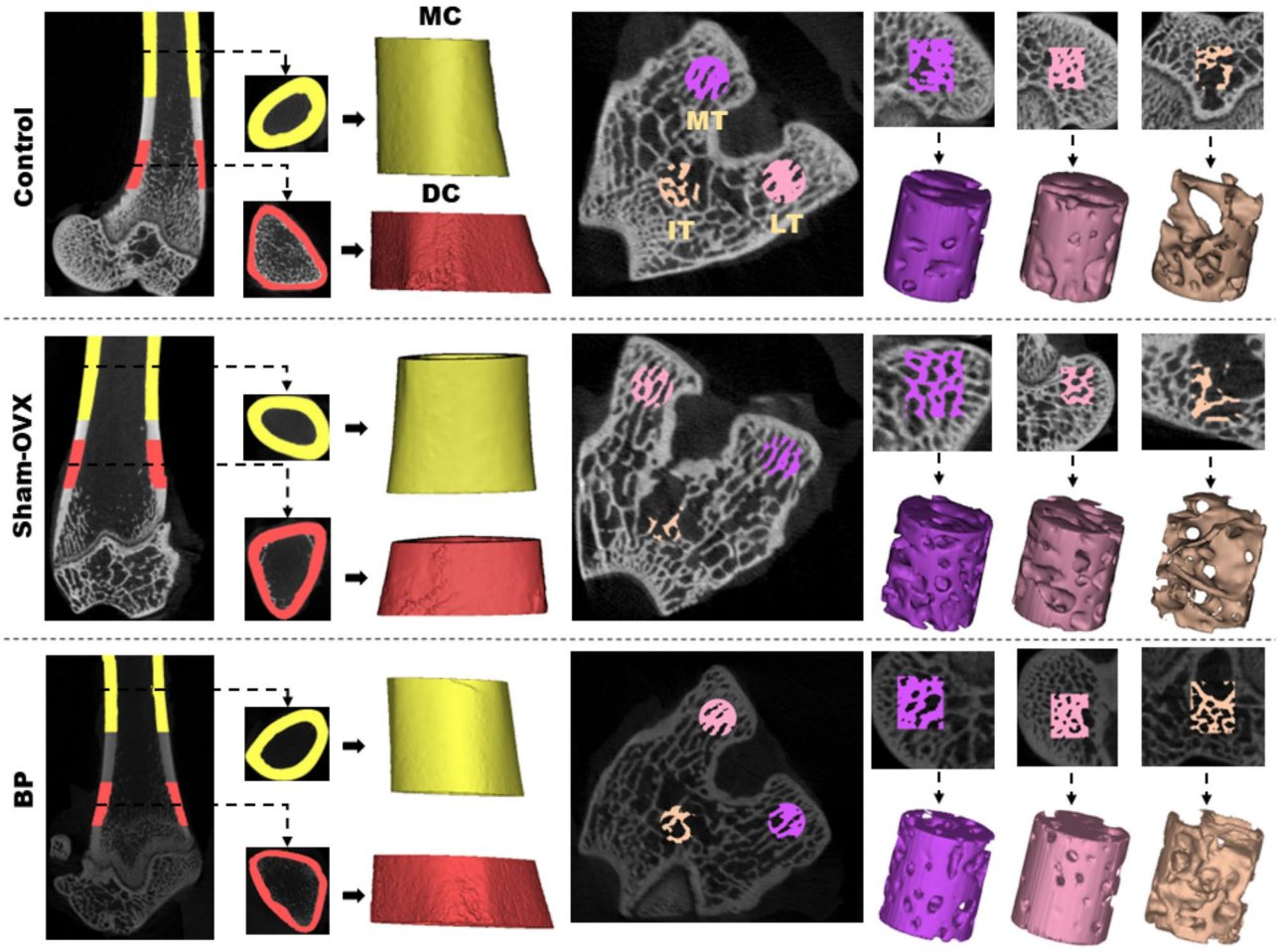

Fig. 2 The construction of 3D models of cortical and trabecular bone in VOI in different groups

Statistical analysis

Statistical analysis was conducted using SPSS Software (SPSS 17.0, IBM, USA). A one-way analysis of variance and post hoc analysis was conducted to compare the groups, and errors were corrected using Tukey's method. The data was presented as mean and standard deviation. $P<0.05$ was considered statistically significant. Linear regression was performed to describe the correlation between the structural parameters and mechanical strength.

Results

Bending performance of tibias

The bending modulus was lower in sham-OVX and BP groups than the normal (sham-OVX vs. Control: $p<0.001$, BP vs. Control: $p<0.001$, sham-OVX vs. BP: $p=0.762$). The deflection was no significant difference in sham-OVX and BP groups (sham-OVX vs. BP: $p=0.306$). The bending strength was lower in sham-OVX group than the BP and Control groups (sham-OVX vs. Control: $p=0.02$, sham-OVX vs. BP: $p=0.041$, BP vs. Control: $p=0.913$). The maximum bending forces were lower in sham-OVX group than the BP and Control groups (sham-OVX vs. Control: $p=0.01$, sham-OVX vs. BP: $p=0.122$, BP vs. Control: $p=0.701$) (Fig. 4).

Microstructural parameters measurement of VOI

The Ct.Th, Ct.Ar/Tt.Ar were higher for the MC than DC, the Ct.Ar, Tt.Ar, were higher for the DC than the MC in three groups. The parameters of Ct.Ar, Ct.Th, Tt.Ar, Ct.Ar/Tt.Ar were almost no significant difference for the MC and DC in three groups (Fig. 5). In IT, the BV/TV (%) was higher in BP group than the sham-OVX ($p<0.001$), and no significant difference compared to the normal group ($p=0.921$), the Tb.Th was no significant difference between the groups, the Tb. N was lower in sham-OVX and BP groups (sham-OVX vs. Control: $p<0.001$, BP vs. Control: $p<0.001$, sham-OVX vs. BP: $p=0.002$), the Tb.Sp was higher for sham-OVX group (sham-OVX vs. Control: $p<0.001$, BP vs. sham-OVX: $p<0.001$, Control vs. BP: $p=0.007$). In MT, the BV/TV (%) was no significant difference between the groups, the Tb.Th was lower in sham-OVX group (sham-OVX vs. Control: $p<0.001$, BP vs. Control: $p=0.003$, sham-OVX vs. BP: $p=0.008$),

Table 1 The porosity calculation of trabecular bone in different groups

Samples	IT			MT			LT		
	BV (mm^3)	BV/TV	1-BV/TV	BV (mm^3)	BV/TV	1-BV/TV	BV (mm^3)	BV/TV	1-BV/TV
Control 1	0.62	0.33	0.67	1.54	0.80	0.20	1.46	0.76	0.24
Control 2	0.70	0.37	0.63	1.52	0.79	0.21	1.25	0.65	0.35
Control 3	0.69	0.36	0.64	1.36	0.71	0.29	1.35	0.70	0.30
Control 4	0.97	0.50	0.50	1.49	0.78	0.22	1.45	0.76	0.24
Control 5	0.65	0.34	0.66	1.11	0.58	0.42	1.37	0.71	0.29
Control 6	0.80	0.41	0.59	1.40	0.73	0.27	1.25	0.65	0.35
Control 7	0.85	0.44	0.56	1.24	0.64	0.36	1.65	0.86	0.14
Control 8	0.87	0.45	0.55	1.47	0.76	0.24	1.37	0.71	0.29
Control 9	0.71	0.37	0.63	1.25	0.65	0.35	1.35	0.71	0.29
Control 10	0.90	0.47	0.53	1.34	0.70	0.30	1.12	0.59	0.41
OVX_{sham} 1	0.42	0.22	0.78	1.40	0.73	0.27	1.36	0.71	0.29
OVX_{sham} 2	0.40	0.21	0.79	1.32	0.69	0.31	1.02	0.53	0.47
OVX_{sham} 3	0.62	0.33	0.67	1.24	0.64	0.36	0.95	0.50	0.50
OVX_{sham} 4	0.30	0.16	0.84	1.56	0.82	0.18	1.02	0.53	0.47
OVX_{sham} 5	0.45	0.23	0.77	1.12	0.59	0.41	1.13	0.59	0.41
OVX_{sham} 6	0.46	0.24	0.76	1.25	0.65	0.35	1.25	0.65	0.35
OVX_{sham} 7	0.44	0.23	0.77	0.85	0.44	0.56	1.33	0.69	0.31
OVX_{sham} 8	0.48	0.25	0.75	1.12	0.59	0.41	1.15	0.60	0.40
OVX_{sham} 9	0.52	0.27	0.73	1.23	0.64	0.36	1.25	0.65	0.35
OVX_{sham}10	0.47	0.24	0.76	0.95	0.50	0.50	1.12	0.59	0.41
BP 1	0.89	0.46	0.54	1.33	0.69	0.31	1.02	0.53	0.47
BP 2	0.64	0.34	0.66	1.25	0.65	0.35	1.37	0.71	0.29
BP 3	0.63	0.33	0.67	1.32	0.69	0.31	1.54	0.80	0.20
BP 4	0.70	0.37	0.63	1.25	0.65	0.35	1.02	0.53	0.47
BP 5	0.77	0.40	0.60	1.46	0.76	0.24	1.46	0.76	0.24
BP 6	0.81	0.42	0.58	1.35	0.71	0.29	1.33	0.69	0.31
BP 7	0.80	0.41	0.59	1.23	0.64	0.36	1.29	0.67	0.33
BP 8	0.80	0.42	0.58	1.12	0.59	0.41	1.15	0.60	0.40
BP 9	0.67	0.35	0.65	1.48	0.77	0.23	1.65	0.86	0.14
BP 10	0.79	0.41	0.59	1.15	0.60	0.40	1.15	0.60	0.40

the Tb.N was lower in sham-OVX group (sham-OVX vs. Control: $p<0.001$, BP vs. Control: $p=0.238$, sham-OVX vs. BP: $p=0.002$), the Tb.Sp was higher for sham-OVX group (sham-OVX vs. Control: $p<0.001$, BP vs. sham-OVX: $p=0.022$, Control vs. BP: $p=0.046$). In LT, the BV/TV (%) was no significant difference in BP and Control groups ($p=0.828$), the Tb.Th was lower in sham-OVX group (sham-OVX vs. Control: $p<0.001$, BP vs. Control: $p=0.004$, sham-OVX vs. BP: $p=0.045$), the Tb.N was no significant difference in BP and Control groups ($p=0.950$), the Tb.Sp was higher in sham-OVX group (sham-OVX vs. Control: $p<0.001$, BP vs. sham-OVX: $p=0.024$, Control vs. BP: $p=0.016$) (Fig. 6).

Effective elastic modulus prediction of VOI models

The stress distribution of MC and DC was shown in Fig. 7A. The predicted effective elastic modulus was higher than the theoretical values, they were no significant difference between the groups (Fig. 7B). The stress distribution of IT, MT, and LT was shown in Fig. 7 C. The predicted effective elastic modulus was lower than the theoretical value. In IT, the predicted modulus of sham-OVX group was lower than the other two groups (sham-OVX PV vs. Control PV: $p<0.001$, sham-OVX PV vs. BPPV: $p<0.001$, BPPV vs. Control PV: $p=0.417$). In MT, the predicted modulus was no significant difference between groups. In LT, the predicted modulus of sham-OVX group was lower than the other two groups (sham-OVX PV vs. Control PV: $p=0.019$, sham-OVX PV vs. BPPV: $p=0.146$, BPPV vs. Control PV: $p=0.996$) (Fig. 7D).

The correlation between microstructural parameters and elastic modulus of VOI

Linear regression was used to predict the relationship between the measured parameters and the effective elastic modulus, positive correlation and good fitness (R^2, from 0.86 to 0.98) were obtained between the measured parameters (Ct.Th, Ct.Ar, Tt.Ar) and the effective elastic modulus of MC and DC in three groups (Fig. 8). In IT,

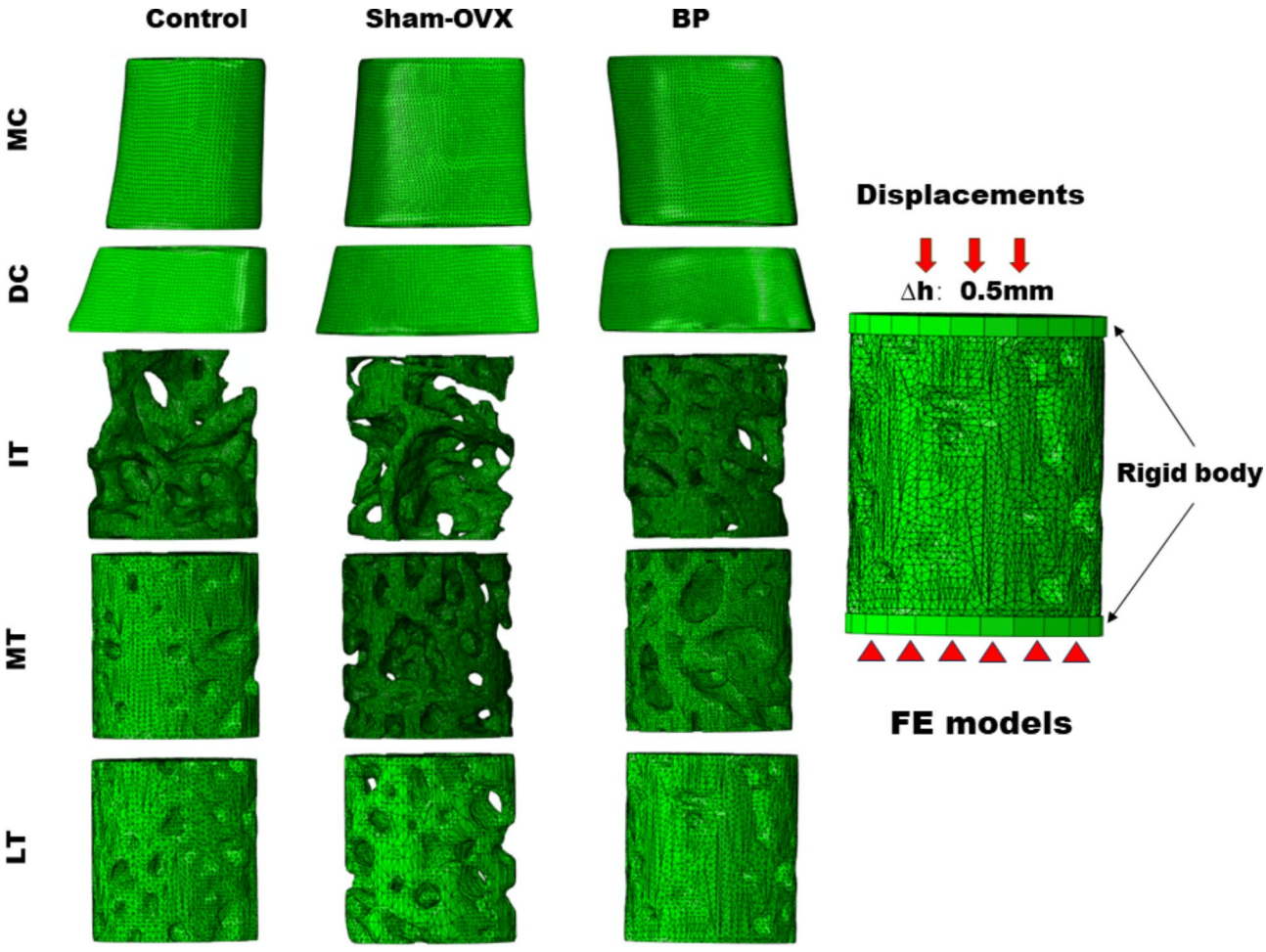

Fig. 3 Finite element models of cortical and trabecular bone in VOI in different groups

positive correlation and good fitness (R^2, from 0.82 to 0.96) were obtained between the measured parameters (BV/TV, Tb.Th, Tb.N) and the effective elastic modulus for three groups. In MT, positive correlation and good fitness (R^2, from 0.73 to 0.98), in LT, positive correlation and good fitness (R^2, from 0.82 to 0.97), were obtained between the measured parameters (BV/TV, Tb.Th) and the effective elastic modulus for three groups. Negative correlation and good fitness (R^2, from 0.83 to 0.96) were obtained between the measured parameters (Tb.Sp) and the effective elastic modulus for three groups in MT (Fig. 9).

Discussion

This study was performed based on micro-CT data of rat femurs, exploring the effects of BPs on the morphological parameters and mechanical strength of cortical and trabecular bone in an animal model of osteoporosis. The results suggested that the effect of BP on cortical bone in osteoporotic rat femurs was not obvious, and even the impact of sham-OVX group on cortical bone. However, BP intervention can significantly promote the morphological structural parameters and mechanical strength of trabecular bone, especially in the non-weight-bearing region (IT), contributing to structural and mechanical reconstruction.

Cortical bone showed a decrease in bone quality and bone mechanical strength in the osteoporotic environment, which may exhibit a certain degree of latency. However, since the duration of this study was relatively short, the impact on cortical bone had not been observed within a short period of time. Similarly, the effect of BP intervention on osteoporotic cortical bone may also have a delayed effect (Figs. 5 and 7B). It is unlikely to cause significant changes in the thickness, area, and mechanical strength of cortical bone in a short period of time. It's been studied the effects of early and late BP treatment on cortical bone of ovariectomized rats were investigated, and the cortical thickness was measured at different time points (4, 8, 12, 16 weeks), indicating that both the sham-OVX and the late BP groups were significantly lower than the early BP group at 4 weeks. However, it increased

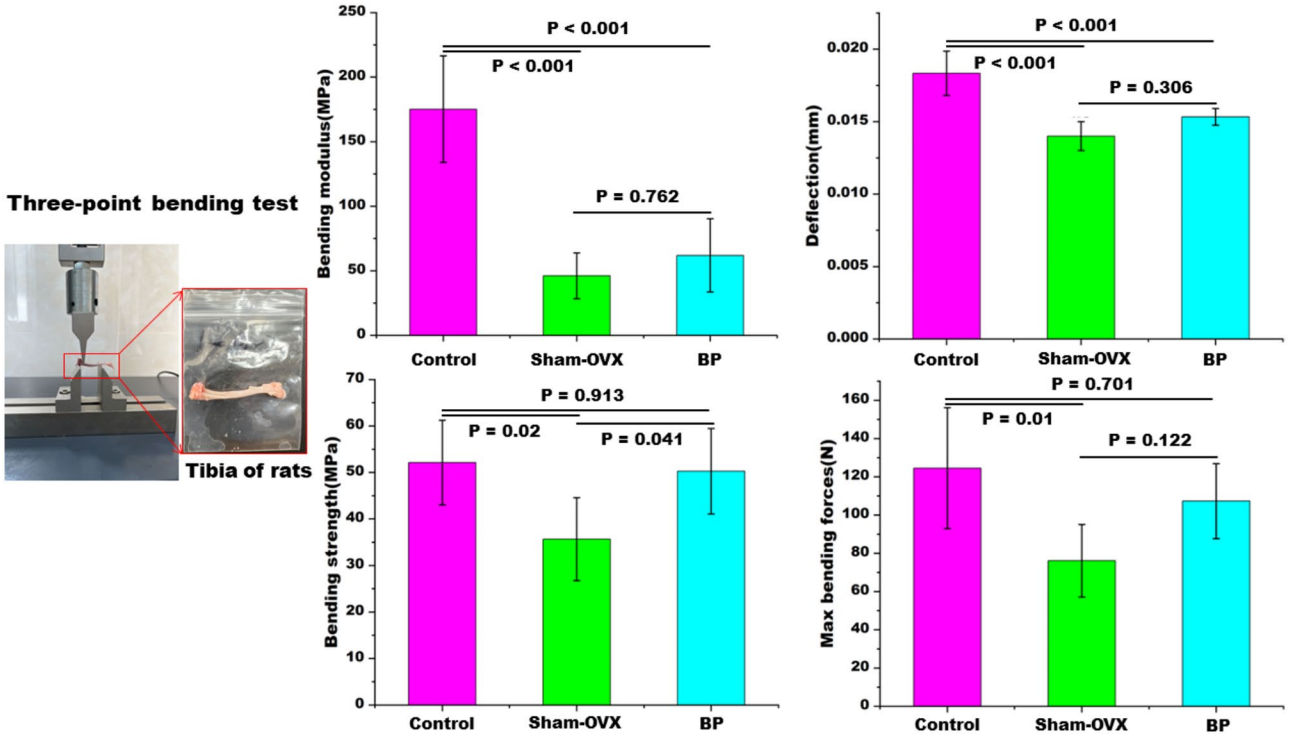

Fig. 4 Three-point bending test of tibias in different groups

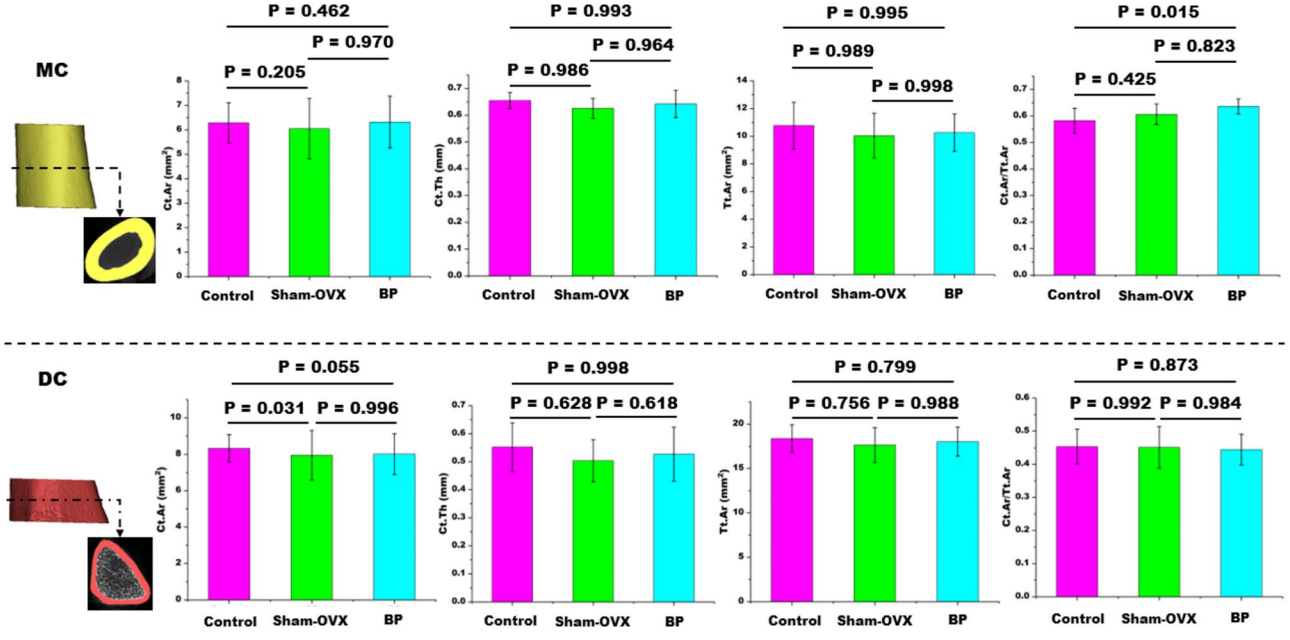

Fig. 5 The structural parameter measurement of cortical bone in VOI in different groups

again in the OVX group after 4weeks, and cortical thickness was significantly higher than in the control group at 16 weeks. Early BP treatment inhibited the changes in cortical thickness. The late BP group, just like the sham-OVX group, showed an increase in cortical thickness between 4 and 16 weeks [20]. Another study found that exercise and BP interacted to synergistically enhance cortical area and thickness of the mid-shaft femur compared to the individual treatments alone after 14 weeks of treatment [21]. It can be seen that the results of different studies on the effect of BP on the cortical thickness of ovariectomized rats are different. Further research

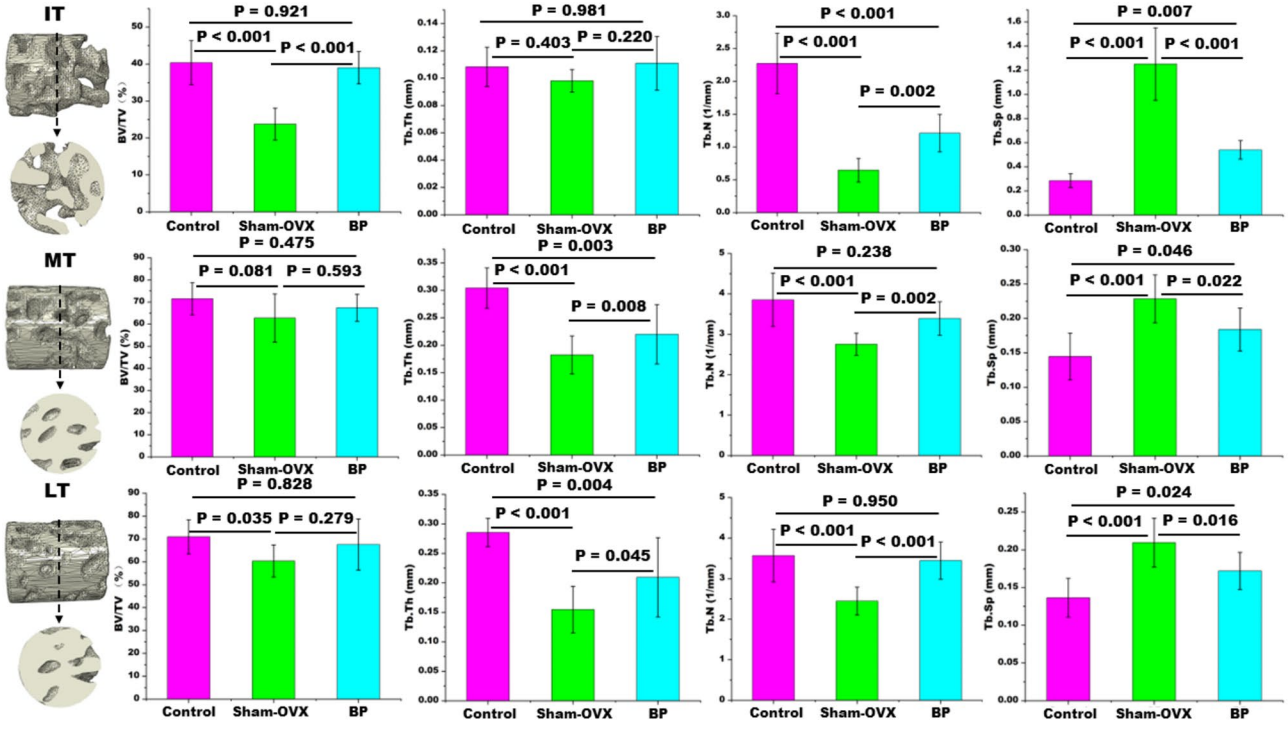

Fig. 6 The structural parameter measurement of trabecular bone in VOI in different groups

is needed to investigate whether it will cause changes in the microscopic structure of cortical bone, such as osteon. As we know, bone remodeling is performed by basic multicellular units (BMUs) that resorb and subsequently form discrete packets of bone tissue [22]. And we can measure the basic multicellular unit activity in cortical bone by 3D morphological analysis in vivo for bone remodeling of osteoporosis and related pharmaceutical treatments [23]. However, from the correlation relationship between cortical bone measurement parameters and the predicted effective elastic modulus (Fig. 8), there was a high positive linear correlation between Ct.Th, Ct.Ar, Tt.Ar, and the effective elastic modulus of cortical bone. Therefore, the mechanical parameters can be evaluated by measuring the structural parameters of cortical bone in the absence of conditions to predict or measure the effective elastic modulus of cortical bone. At the same time, the linear correlation stability of cortical bone was better than the predicted results of trabecular bone in different groups.

Based on this, it can be observed from the three-point bending test of the tibia that BP can significantly improve the bending strength and maximum bending force of the femur in osteoporotic rats. According to the report, it's been studied the femoral midshaft strength and ultimate load by three-point bending to failure, the femoral midshaft ultimate load was significantly higher in animals treated with BP than in the sham-OVX group. The femoral midshaft strength was also significantly reduced in ovariectomized animals to the controls and the BP treatment resulted in significantly increased strength over the sham-OVX group [24], which was consistent with the results in this study. However, there was no benefit in improving the bending modulus and deflection (Fig. 4). The reason may be that the impact of osteoporosis on Ct.Th, Ct.Ar was not obvious, resulting in no significant difference in the calculated results of effective bending modulus and deflection among the groups.

Compared to cortical bone, this research focused more on the effects of osteoporosis and BP on trabecular bone. Indeed, there have been numerous reports on the impact of osteoporosis and related pharmaceutical treatments on trabecular bone [25–27]. However, this study's interesting finding was that osteoporosis significantly altered the trabecular bone structure parameters in IT, while having a lesser effect on the structure MT and LT. Similarly, BPs can improve BV/TV, Tb. N, and reduce Tb.Sp in IT. However, the impact on the structural parameters in MT and LT was smaller than that of the IT (Fig. 6). In fact, from the perspective of bone histomorphometry, BP did not cause significant improvement for all measured parameters, which largely depended on the duration and time points (for example: early or late after OVX) of BP intervention. According to the study report, the early BP treatment and control groups were not significantly different at all time points for all structural parameters. The BV/TV, and Tb.N were significantly different between all groups except for the early treatment and control groups

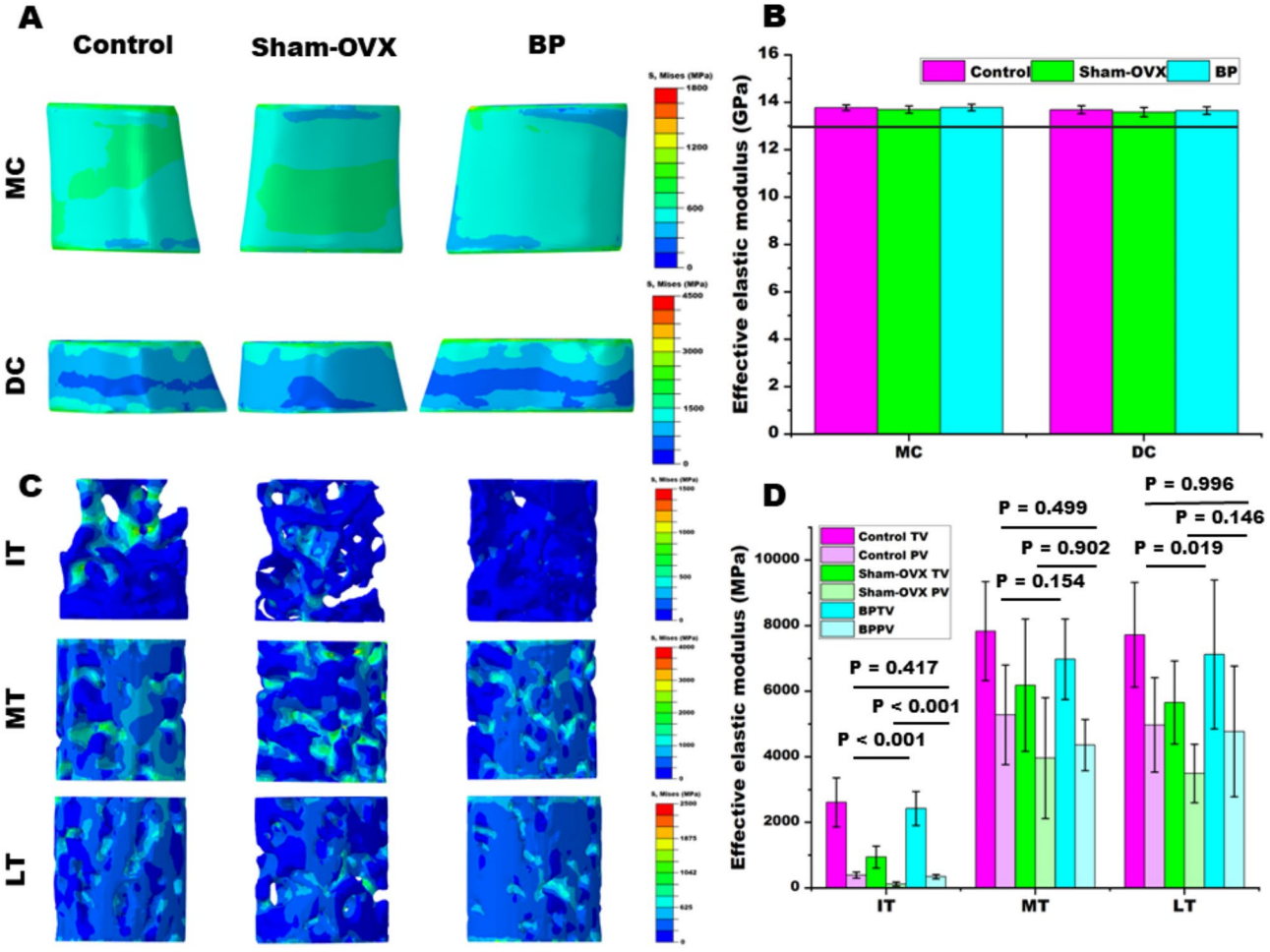

Fig. 7 Mechanical property prediction for cortical and trabecular bone in different groups. The stress distribution of cortical bone (**A**). The effective elastic modulus prediction for cortical bone (**B**). The stress distribution of trabecular bone (**C**). The effective elastic modulus prediction for trabecular bone (**D**). Control TV: control theoretical value, Control PV: control predicted value, sham-OVX TV: ovariectomy theoretical value, sham-OVX PV: ovariectomy predicted value, BPTV: bisphosphonates theoretical value, BPPV: bisphosphonates predicted value

at week 16 [20]. From osteoporotic human specimens study, the BV/TV and Tb.Th were significantly greater in BP specimens, and Tb.Sp was significantly smaller after three years BP treatments [28].

This was also supported by the mechanical prediction, as BP significantly improved the effective elastic modulus of trabecular bone in IT compared to MT and LT (Fig. 7D). We speculated that this result may be due to the lower stress experienced by the IT compared to the medial and lateral condyles, even more, combined with the osteoporotic environment, which easily leads to a decrease in BV/TV. On the other hand, the trabecular bone structures on both femoral condyles were in a weight-bearing position, and according to Wolff's law, it may compensate for the stress by increasing the BV/TV. According to the literature, the consensus of most studies, both those based on ovariectomized and intact animal models on testing of human bone, is that long-term treatment and/or high does with certain BP makes the bone tissue more brittle and less tough. This translates into reduced energy to fracture and potentially a shorter bone fatigue life [29]. On the other hand, the changes in apparent stiffness and failure stress are attributable to changes in trabecular bone structure, which in turn are related to the duration of BP treatment and the optimal BP therapy duration await study of additional bone quality parameters [30]. The bone modulus increases with BP treatment duration up to 6 years, no additional modulus increases occurred after 6 years of treatment. Although strength increased, peaked at 12.4 years and remained constant for the next 7.6 years of BP treatment, and the effectiveness of BP treatment was not obvious at the early stage [31], which may explain why a lack of statical significance in structural and mechanical parameters between sham-OVX and BP treatment groups.

The limitations of this study were as follows: (1) Although the finite element model in this study had been well validated, there is no specific feasible

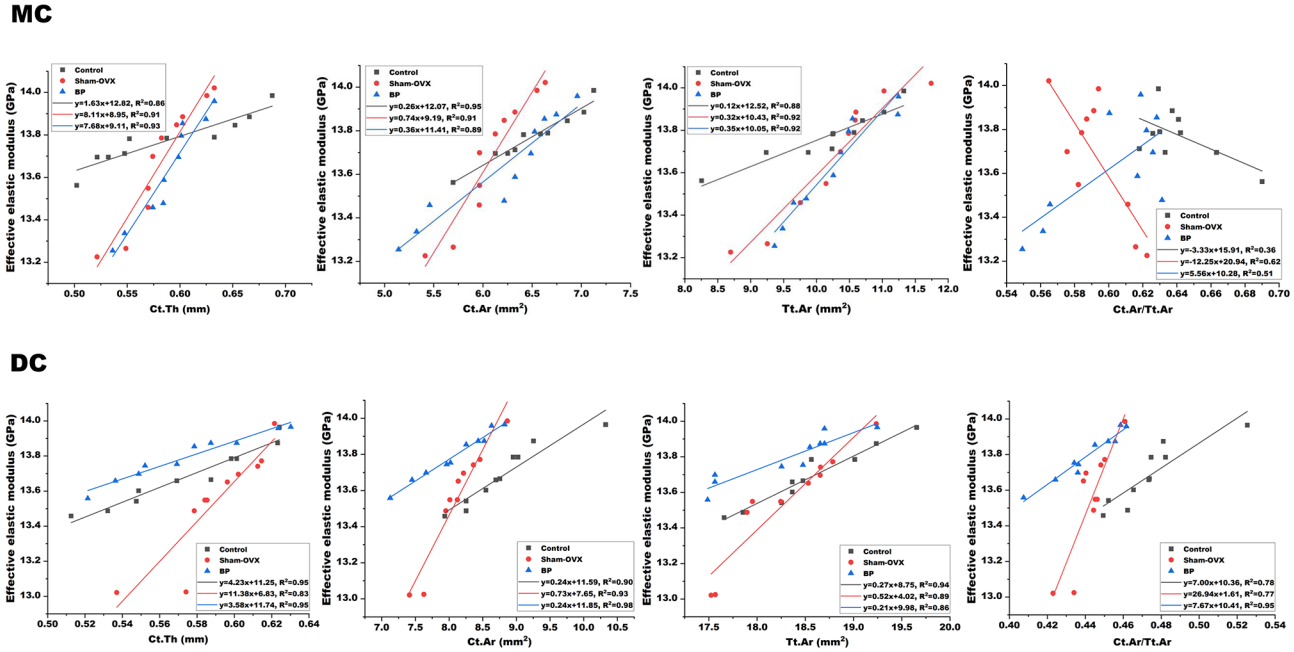

Fig. 8 The correlation relationship prediction between the structural parameters and effective elastic modulus for cortical bone

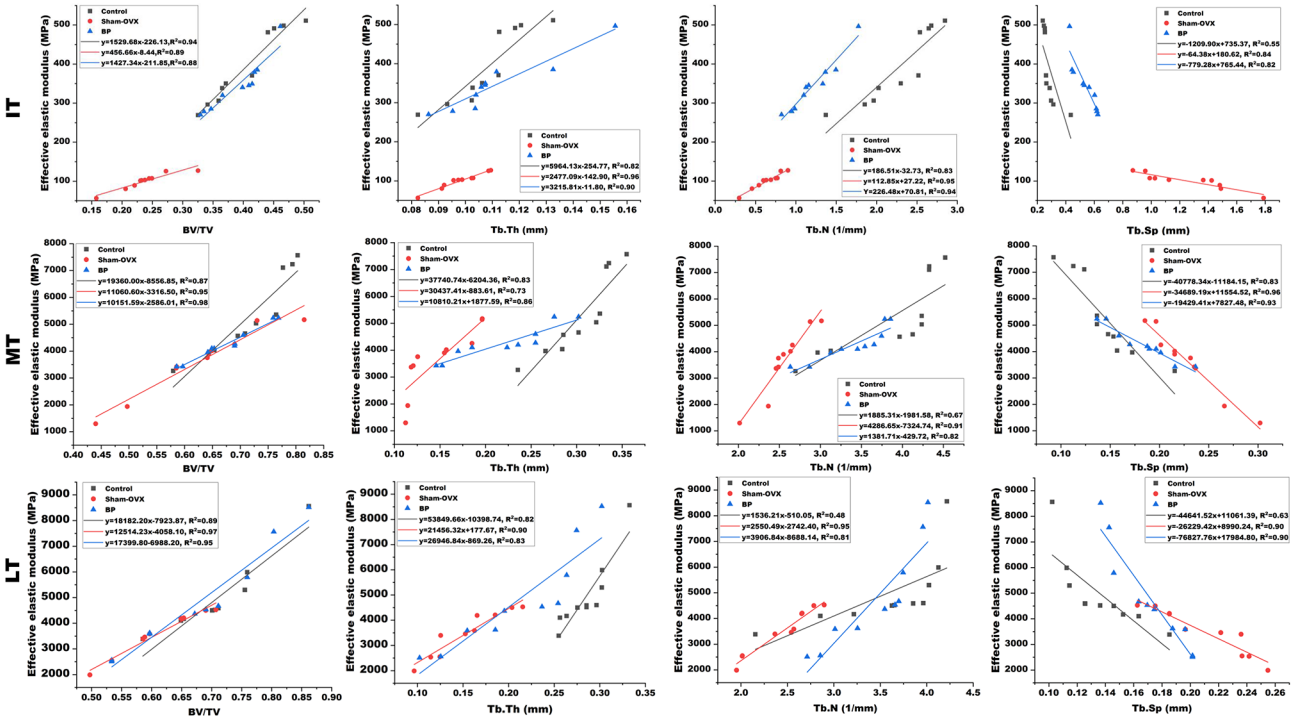

Fig. 9 The correlation relationship prediction between the structural parameters and effective elastic modulus for trabecular bone

solution for validating the cortical and trabecular bone in vivo or in vitro under real mechanical environments, currently [32]. Due to the differences in material properties of 3D printed specimens, there is a certain difference between the mechanical properties determined by in vitro mechanical tests and the actual bone structure mechanical parameters. Therefore, in the future, improving the in vivo measurement and data collection of animal models, such as combining the technology of cellular mechanics, will be the research direction. (2) Due to the small samples and short study period in this study, as well as individual differences, the measurement results may

be affected, especially the instability of trabecular bone structure among samples within the same group, leading to certain deviations in data analysis of inter-group measurements. Increasing the samples and extending the study period may improve the reliability of the research results.

Conclusion

This study was the first to explore the different effects of BP on the microstructure and mechanical properties of cortical and trabecular bone in an osteoporotic model. In the short study term, the intervention of BP had minimal impact on the Ct.Th, Ct.Ar, and effective elastic modulus of cortical bone. Additionally, there was a good positive linear correlation between structural parameters and the effective elastic modulus. In comparison, the intervention of BP on trabecular bone showed differences. However, it significantly improved the BV/TV and effective elastic modulus of the trabecular bone in IT. On the other hand, the structure parameters and effective elastic modulus of trabecular bone in the both femoral condyles may be improved through stress compensation to counteract the decrease in bone quality and mechanical strength caused by osteoporosis. This provided a new treatment approach for the prevention of osteoporotic fractures in clinical practice.

Abbreviations

OP	Osteoporosis
SD	Sprague–Dawley
OVX	Ovariectomy
BP	Bisphosphonate
SPF	Specific-pathogen-free
VOI	Volume of interest
Ct.Th	Cortical thickness
Ct.Ar	Cortical area
Tt.Ar	Total area
Ct.Ar/Tt.Ar	The ratio of cortical area and total area
BV/TV	Bone volume fraction
Tb.Th	Trabecular thickness
Tb.N	Trabecular number
Tb.Sp	Trabecular separation
DICOM	Digital Imaging and Communications in Medicine
Control TV	Control theoretical value
Control PV	Control predicted value
OPTV	Osteoporosis theoretical value
OPPV	Osteoporosis predicted value
BPTV	Bisphosphonates theoretical value
BPPV	Bisphosphonates predicted value
BMUs	Basic multicellular units

Acknowledgements

I would like to thank the professors of the Pharmacological Medical Research Center of Zhongshan Hospital of Traditional Chinese Medicine Affiliated to Guangzhou University of Traditional Chinese Medicine for their guidance and provision of experimental sites and equipment for this study.

Author contributions

Conceptualization: Yz W; methodology: Yz W; software: Yz W; validation: ZW and DG; formal analysis: MW; investigation: ZW; resources: Yz W; data curation: Yf W; writing—original draft preparation: Yz W; writing—review and editing: Yz W, ZW and CL; visualization: CM and JC; supervision: MW and HW; project administration: Yz W; funding acquisition: Yz W. All authors have read and agreed to the published version of the manuscript.

Funding

This work was supported by the Youth Project of Guangzhou Science and Technology Bureau (NO. 2023A04J1838), Medical research project of Zhongshan (NO. 2023A020455), and President's fund of The Fifth Affiliated Hospital of Southern Medical University (NO. YZ2022QN05). The funders had no role in design of the study, the collection, analysis, and interpretation of the data, or in writing the manuscript.

Data availability

The data and materials are available from the corresponding author.

Declarations

Ethics approval and consent to participate

The animal research protocol was approved by the ethics committee of Zhongshan Hospital of Traditional Chinese Medicine Affiliated to Guangzhou University of Traditional Chinese Medicine (NO. AEWC-2023008). And the animals were obtained from Guangdong Medical Animal Laboratory Center for medical research.

Consent for publication

Not applicable.

Competing interests

The authors declare no competing interests.

Received: 4 May 2024 / Accepted: 4 September 2024
Published online: 10 September 2024

References

1. Carey JJ, Chih-Hsing Wu P, Bergin D. Risk assessment tools for osteoporosis and fractures in 2022. Best Pract Res Clin Rheumatol. 2022;36(3):101775.
2. Chen X, Hua W, Huang X, Chen Y, Zhang J, Li G. Regulatory Role of RNA N6 methyladenosine modification in Bone Biology and osteoporosis. Front Endocrinol (Lausanne). 2020;10:911.
3. Yong EL, Logan S. Menopausal osteoporosis: screening, prevention and treatment. Singap Med J. 2021;62(4):159–66.
4. Gehrke B, Alves Coelho MC, Brasil d'Alva C, Madeira M. Long-term consequences of osteoporosis therapy with bisphosphonates. Arch Endocrinol Metab. 2023;68:e220334.
5. Drake MT, Clarke BL, Khosla S. Bisphosphonates: mechanism of action and role in clinical practice. Mayo Clin Proc. 2008;83(9):1032-45.
6. Smith MR. Osteoporosis and other adverse body composition changes during androgen deprivation therapy for prostate cancer. Cancer Metastasis Rev.,2002;21(2):159-66.
7. Mys K, Varga P, Gueorguiev B, Hemmatian H, Stockmans F, van Lenthe GH. Correlation Between Cone-Beam Computed Tomography and High-Resolution Peripheral Computed Tomography for Assessment of Wrist Bone Microstructure. J Bone Miner Res.2019;34(5):867 – 74.
8. Peyrin F, Dong P, Pacureanu A, Langer M. Micro- and nano-CT for the study of bone ultrastructure. Curr Osteoporos Rep. 2014;12(4):465–74.
9. MacNeil JA, Boyd SK. Accuracy of high-resolution peripheral quantitative computed tomography for measurement of bone quality. Med Eng Phys. 2007;29(10):1096–105.
10. Burr DB. The use of finite element analysis to estimate the changing strength of bone following treatment for osteoporosis. Osteoporos Int. 2016;27(9):2651–4.
11. Ohs N, Collins CJ, Atkins PR. Validation of HR-pQCT against micro-CT for morphometric and biomechanical analyses: a review. Bone Rep. 2020;13:100711.
12. Chen T, Chen M, Yao X, Long W, Chen H, Li L. A new three-point bending test for bone biomechanical properties of rat's tibia. Sheng Wu Yi Xue Gong Cheng Xue Za Zhi. 2008;25(2):341–5.
13. Rovaris K, Queiroz PM, Vasconcelos KF, Corpas LDS, Silveira BMD, Freitas DQ. Segmentation methods for Micro CT images: a comparative study using human bone samples. Braz Dent J. 2018;29(2):150–3.

14. Bouxsein ML, Boyd SK, Christiansen BA, et al. Guidelines for assessment of bone microstructure in rodents using micro-computed tomography. J Bone Min Res. 2010;25(7):1468–86.
15. Mehboob H, Tarlochan F, Mehboob A, Chang SH, Ramesh S, Harun WSW, Kadirgama K. A novel design, analysis and 3D printing of Ti-6Al-4V alloy bio-inspired porous femoral stem. J Mater Sci Mater Med. 2020;31(9):78.
16. Wu X, Gong H, Hu X, Shi P, Cen H, Li C. Effect of verapamil on bone mass, microstructure and mechanical properties in type 2 diabetes mellitus rats. BMC Musculoskelet Disord. 2022;23(1):363.
17. Zheng L, Dai Y, Zheng Y, He X, Wu M, Zheng D, Li C, Fan Y, Lin Z. Medial tibial plateau sustaining higher physiological stress than the lateral plateau: based on 3D printing and finite element method. Biomed Eng Online. 2022;21(1):68.
18. Wang Y, Yamako G, Okada T, Arakawa H, Nakamura Y, Chosa E. Biomechanical effect of intertrochanteric curved varus osteotomy on stress reduction in femoral head osteonecrosis: a finite element analysis. J Orthop Surg Res. 2021;16(1):465.
19. Wang M, Wang Y, Meng Y, Chenglong P. Functionally graded stem optimizes the fixed and sliding surface coupling mechanism. Comput Methods Biomech Biomed Engin. 2023:1–13.
20. Brouwers JE, Lambers FM, Gasser JA, van Rietbergen B, Huiskes R. Bone degeneration and recovery after early and late bisphosphonate treatment of ovariectomized wistar rats assessed by in vivo micro-computed tomography. Calcif Tissue Int. 2008;82(3):202–11.
21. Fuchs RK, Shea M, Durski SL, Winters-Stone KM, Widrick J, Snow CM. Individual and combined effects of exercise and alendronate on bone mass and strength in ovariectomized rats. Bone. 2007;41(2):290–6.
22. Loundagin LL, Cooper DML. Towards novel measurements of remodeling activity in cortical bone: implications for osteoporosis and related pharmaceutical treatments. Eur Cell Mater. 2022;43:202–27.
23. Loundagin LL, Harrison KD, Wei X, Cooper DML. Understanding basic multicellular unit activity in cortical bone through 3D morphological analysis: new methods to define zones of the remodeling space. Bone. 2024;179:116960.
24. Lauritzen DB, Balena R, Shea M, Seedor JG, Markatos A, Le HM, Toolan BC, Myers ER, Rodan GA, Hayes WC. Effects of combined prostaglandin and alendronate treatment on the histomorphometry and biomechanical properties of bone in ovariectomized rats. J Bone Min Res. 1993;8(7):871–9.
25. Li J, Hu Y, You H, Li R, Ran Q, Ouyang T, Huang Y. Trabecular bone microarchitecture evaluation in an osteoporosis mouse model. J Vis Exp. 2023;(199).
26. Huang X, Zheng L, Zheng D, Li S, Fan Y, Lin Z, Huang S. Studying trabecular bone samples demonstrates a power law relation between deteriorated structure and mechanical properties - a study combining 3D printing with the finite element method. Front Endocrinol (Lausanne). 2023;14:1061758.
27. Wang SP, Chen YJ, Hsu CE, Chiu YC, Tsai MT, Hsu JT. Intermittent parathyroid hormone treatment affects the bone structural parameters and mechanical strength of the femoral neck after ovariectomy-induced osteoporosis in rats. Biomed Eng Online. 2022;21(1):6.
28. Recker R, Masarachia P, Santora A, Howard T, Chavassieux P, Arlot M, Rodan G, Wehren L, Kimmel D. Trabecular bone microarchitecture after alendronate treatment of osteoporotic women. Curr Med Res Opin. 2005;21(2):185–94.
29. Burr DB. Fifty years of bisphosphonates: what are their mechanical effects on bone? Bone. 2020;138:115518.
30. Ward J, Wood C, Rouch K, Pienkowski D, Malluche HH. Stiffness and strength of bone in osteoporotic patients treated with varying durations of oral bisphosphonates. Osteoporos Int. 2016;27(9):2681–8.
31. Pienkowski D, Wood CL, Malluche HH. Young's modulus and hardness of human trabecular bone with bisphosphonate treatment durations up to 20 years. Osteoporos Int. 2019;30(2):277–85.
32. Guha I, Zhang X, Rajapakse CS, Letuchy EM, Chang G, Janz KF, Torner JC, Levy SM, Saha PK. Computed tomography-based stiffness measures of trabecular bone microstructure: cadaveric validation and in vivo application. JBMR Plus. 2022;6(6):e10627.

Publisher's note